Cell PRESS
Cell Host & Microbe
Resource

An In Vivo RNAi Screening Approach to Identify Host Determinants of Virus Replication

Andrew Varble,[1] Asiel A. Benitez,[1] Sonja Schmid,[1] David Sachs,[2] Jaehee V. Shim,[1] Ruth Rodriguez-Barrueco,[5] Maryline Panis,[1] Marshall Crumiller,[3] Jose M. Silva,[5] Ravi Sachidanandam,[2] and Benjamin R. tenOever[1,4,*]
[1]Department of Microbiology
[2]Department of Genetics and Genomic Sciences
[3]Fishberg Department of Neuroscience and Friedman Brain Institute
[4]Global Health and Emerging Pathogens Institute
Icahn School of Medicine at Mount Sinai, New York, NY 10029, USA
[5]Herbert Irving Comprehensive Cancer Center, Columbia University College of Physicians and Surgeons, Columbia University, New York, NY 10032, USA
*Correspondence: benjamin.tenoever@mssm.edu
http://dx.doi.org/10.1016/j.chom.2013.08.007

SUMMARY

RNA interference (RNAi) has been extensively used to identify host factors affecting virus infection but requires exogenous delivery of short interfering RNAs (siRNAs), thus limiting the technique to non-physiological infection models and a single defined cell type. We report an alternative screening approach using siRNA delivery via infection with a replication-competent RNA virus. In this system, natural selection, defined by siRNA production, permits the identification of host restriction factors through virus enrichment during a physiological infection. We validate this approach with a large-scale siRNA screen in the context of an in vivo alphavirus infection. Monitoring virus evolution across four independent screens identified two categories of enriched siRNAs: specific effectors of the direct antiviral arsenal and host factors that indirectly dampened the overall antiviral response. These results suggest that pathogenicity may be defined by the ability of the virus to antagonize broad cellular responses and specific antiviral factors.

INTRODUCTION

The cellular response to virus infection in vertebrates relies on an extensive signaling network that culminates in the production of antiviral cytokines and upregulation of hundreds of antiviral gene products (tenOever, 2013). With respect to RNA viruses, cellular detection is the result of RNA structures foreign to the cell including double-stranded RNA and RNA with exposed 5′ triphosphates (Kolakofsky et al., 2012). Detection of these genetic structures, commonly referred to as pathogen-associated molecular patterns (PAMPs), is mediated by pathogen recognition receptors (PRRs), such as RIG-I and MDA5 (Loo and Gale, 2011; Takeuchi and Akira, 2008). PRR engagement results in recruitment to the mitochondria and subsequent assembly of many host factors including the mitochondrial antiviral signaling protein (MAVS, also called IPS-1, VISA, and Cardiff), as well as a number of Traf family members (McWhirter et al., 2005). MAVS engagement coordinates the activation of NF-κB and IRFs through the IKK and IKK-related kinases, respectively, resulting in the assembly of the IFNβ (Ifnb) enhancesome and subsequent gene induction (McWhirter et al., 2005). IFNβ, a type I IFN (IFN-I), leads to upregulation of hundreds of IFN-stimulated genes (ISGs), which together cooperate to slow virus replication (Li et al., 2013; Schoggins et al., 2011).

Many ISGs and virus host factors have been identified as a result of RNAi screening. High-throughput screens have been used to investigate a myriad of host factors that impact the replication capacity of influenza A virus (IAV), dengue virus, hepatitis C virus (HCV), West Nile virus (WNV), and human immunodeficiency virus (HIV) (Brass et al., 2008; König et al., 2008, 2010; Krishnan et al., 2008; Li et al., 2009; Sessions et al., 2009). These screens have yielded valuable insights into virus-host interactions, yet they all demand the use of in vitro cell cultures and an indirect measure of virus output (i.e., luciferase or cell surface staining). Consequently, efforts are being undertaken to study infections in their physiological context by monitoring genomic polymorphisms between outbred mice and correlating these to virus susceptibility (Ferris et al., 2013). In an effort to expand upon the findings of traditional in vitro siRNA approaches, we sought to adapt this screening platform to an in vivo infection, thereby eliminating the need for a transformed cell line and allowing the direct measure of viral output. To this end, we combined the silencing potential of whole-genome siRNA libraries with the capacity of viruses to produce functional microRNAs (miRNAs).

The discovery that small RNAs (sRNAs) between 19 and 22 nucleotides (nt) in length have the capacity to silence host transcripts ushered in a new era for molecular biology (Bartel, 2004). Generally referred to as RNA interference (RNAi), the silencing potential of sRNAs is largely an attribute to the amount of complementarity between sRNA and mRNA (Bartel, 2004). Endogenous miRNA posttranscriptional silencing (PTS) typically results in "fine-tuning" of target expression with changes of less

than 2-fold observed at the level of protein (Bartel, 2004). However, the silencing capacity of miRNAs can match the ability of siRNAs to enzymatically cleave transcripts, if either the target transcript or the miRNA itself is modified to achieve perfect complementarity (Zeng et al., 2002). Given the silencing potential of sRNAs, numerous viruses have been shown to utilize this form of posttranscriptional regulation to create a more favorable replication environment (Cullen, 2011). Perhaps not surprisingly, virus utilization of miRNAs has been limited to those that replicate in the nucleus and persist for extended periods of time (Cullen, 2011). Furthermore, despite extensive sequencing efforts, no RNA virus, void of a DNA intermediate, has been found to encode a canonical miRNA (Kincaid et al., 2012; Parameswaran et al., 2010; Perez et al., 2009; Pfeffer et al., 2004; tenOever, 2013). However, lack of endogenous evidence for RNA virus-mediated miRNA production is not indicative of an inherent constraint. This is perhaps best exemplified by the fact that we and others, have demonstrated that RNA viruses, regardless of genome polarity or site of replication, can be engineered to generate such products (Langlois et al., 2012; Rouha et al., 2010; Shapiro et al., 2010, 2012; Varble et al., 2010).

Here we describe an RNAi-based approach to identify interactions between virus and host that impact overall replication in the context of an in vivo infection. This is achieved by enabling siRNA delivery through a replication-competent alphavirus. To this end, we generated a Sindbis-based library of viruses that are identical at a protein level, but each virion encodes a unique siRNA capable of silencing a single open reading frame (ORF). These libraries were subjected to a selective pressure to parse out those host factors that enhance replication. Screening both in vitro and in vivo corroborated a number of known antiviral host factors but also identified ORFs that, when silenced, resulted in enhanced virus replication. These data suggest that virus replication and pathogenicity may be the product of more than the known antiviral host genes and provides insights into other factors that may be the target of viral antagonists.

RESULTS

Sindbis Virus-Mediated Silencing of GFP

With the knowledge that RNA viruses have the capacity to elicit PTS, we utilized a miR-30-based whole-genome-targeting library (Silva et al., 2005) to probe for virus-host interactions using the pathogen as the siRNA delivery mechanism. Given that a natural infection results in viral quasispecies that provide the ability to adapt to the host response (Vignuzzi et al., 2006), we reasoned that a library of engineered viruses, each equipped to silence one host factor, may mimic this selection process. To this end, we generated a large cohort of attenuated and mouse-adapted Sindbis viruses (SINV), each designed to produce an artificial miRNA (amiRNA) and monitored selection in vivo (Figure S1A).

To demonstrate the capacity of SINV to act as a platform for amiRNA delivery, we designed a collection of five unique hairpins targeting enhanced green fluorescent protein (GFP). Accurate processing and PTS of these amiRNAs was confirmed by small RNA northern blot and western blot, respectively (Figures S1B and S1C). These data demonstrate four of the five hairpins effective in silencing GFP, with two hairpins showing complete knockdown (Figure S1C). To ascertain whether incorporation of a GFP amiRNA conferred silencing activity onto SINV, amiRNA-GFP^{122}, which was designed to conform to the structure of miR-124 (Figure 1A), was inserted into the recombinant SINV. As previously described (Shapiro et al., 2010, 2012), despite the cytoplasmic replication of SINV, amiRNA-GFP^{122} demonstrated accurate processing and robust expression at every time point evaluated following SINV-amiRNA-GFP infection (Figure 1B). More importantly, the capacity to generate the amiRNA also enabled the virus to silence GFP expression in the context of infection (Figure 1C).

Targeting ISGs In Vitro Provides Enhanced Virus Replication

Given the capacity to confer GFP silencing potential onto SINV, we next sought to determine whether silencing of an ISG could enhance overall replication. To this end, we designed an amiRNA library to a subset of ISGs, targeting each ORF with two distinct hairpins (Table S1). These amiRNAs were individually generated following the same strategy as SINV-amiRNA-GFP (Figure 1A). Quadruplicate passaging in vitro showed evidence for positive selection of viruses targeting: IKKβ (*Ikbkb*) and RIG-I (*Ddx58*) (Figure S2A). Among the enriched amiRNAs, identification of two independent siRNAs silencing RIG-I prompted us to characterize a *Ddx58*-targeting virus further (Figure 2A). Given that RIG-I has not been directly implicated in SINV detection, we first used an independent siRNA to silence this factor in vitro (Figure S2B). In agreement with data implicating RIG-I sensing for Chikungunya virus, a related alphavirus (Schilte et al., 2010), we found a significant enhancement of virus replication as a result of in vitro RIG-I silencing (Figure S2C). Furthermore, we compared virus titers in wild-type and *Ddx58*$^{-/-}$ fibroblasts and corroborated the RNAi data, finding virus levels were elevated by more than one log in the absence of this PRR (Figure S2D). Following this observation, we engineered SINV to express an amiRNA designed to silence murine RIG-I (SINV-amiRNA-RIG-I) and compared this to a control SINV strain encoding a nonspecific amiRNA (SINV-amiRNA-Ctrl). Cell culture infections comparing the control virus (SINV-Ctrl) to SINV-amiRNA-RIG-I demonstrated accurate processing of the amiRNA and the capacity to diminish RIG-I protein expression (Figures S2E and 2B). Not surprisingly, the amiRNA-RIG-I also conferred a replicative advantage to this attenuated SINV strain, as virus levels were an order of magnitude higher compared to a matched control virus (SINV-Ctrl) (Figure 2C). Improved levels of replication were the direct result of amiRNA-mediated targeting, as this phenotype was lost in cells lacking the capacity to generate miRNAs due to Dicer deficiency (Figures S2F and S2G).

Small RNA-Mediated Natural Selection In Vivo

Given the replicative advantage conferred onto SINV through use of an encoded amiRNA, we utilized a small collection of viruses containing unique hairpins to determine whether natural selection would parse out advantageous noncoding RNAs in the context of an in vivo infection and ascertain the timing of enrichment. This initial SINV library was composed of approximately 4,000 unique hairpins, each designed to target a murine ORF (Silva et al., 2005). Population infection experiments, followed by small RNA cloning and deep sequencing analysis, demonstrated approximately 75% of the amiRNAs were processed as

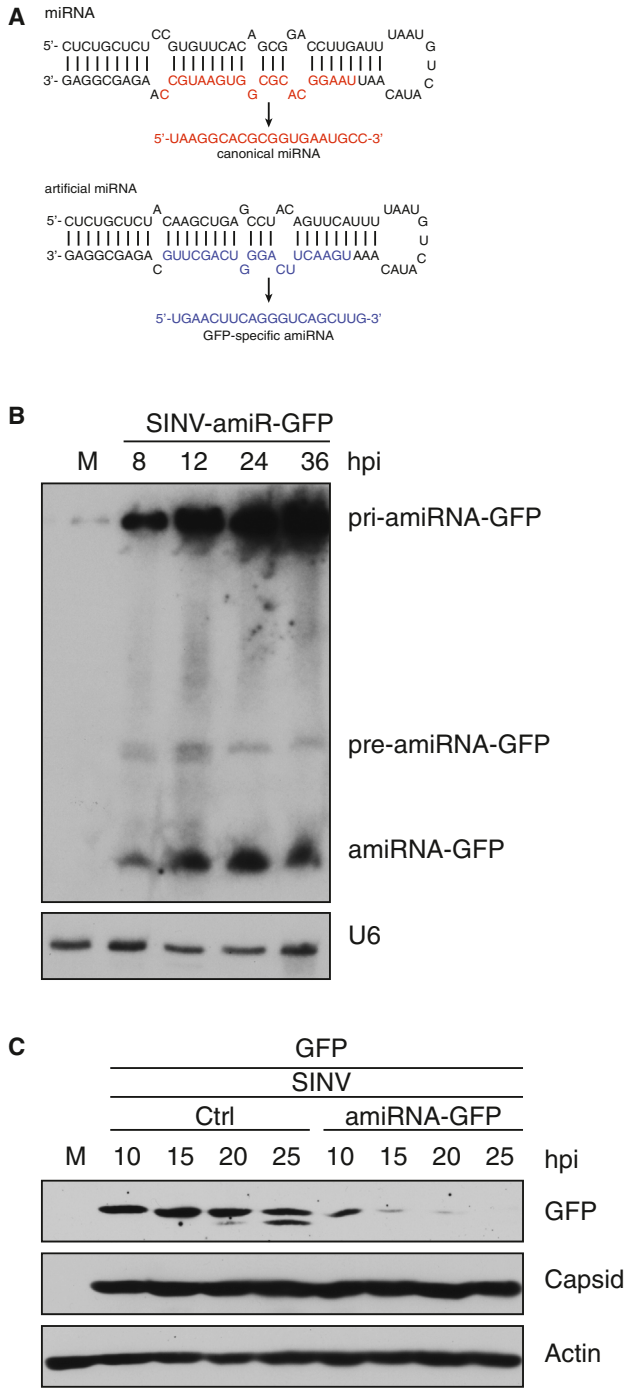

Figure 1. Functional amiRNA Production from Sindbis Virus

(A) Schematic depicting the native mmu-miR-124-2 hairpin (top) followed by a modified hairpin designed to target GFP (bottom).

(B) Small RNA northern blot of RNA derived from BHK cells infected with SINV (moi = 1) expressing an amiRNA designed to silence GFP (SINV-amiRNA-GFP). Blots were probed for the amiRNA and U6 at indicated time points.

(C) Western blot analysis of whole-cell extract derived from SINV-Ctrl and SINV-amiRNA-GFP-infected BHK cells (moi = 2) expressing pEGFP. Blots depict GFP, SINV capsid, and actin. See also Figure S1.

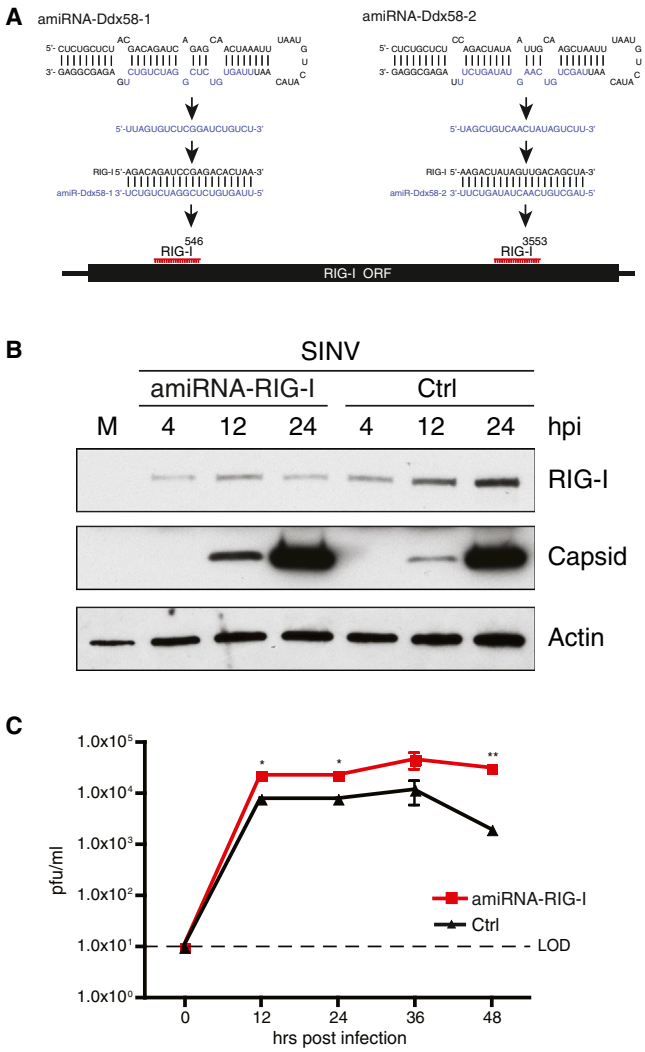

Figure 2. SINV Replication Can Be Modulated by amiRNA Expression

(A) Schematic depicting the mmu-miR-124-2 hairpins modified to target RIG-I selected for during in vitro passaging.

(B) Western blot analysis of whole-cell extract derived from murine embryonic fibroblasts (MEFs) infected with SINV-RIG-I or -Ctrl (moi = 0.01). Blots depict RIG-I, SINV capsid, and actin.

(C) Multicycle growth curve of viruses in (B). Data are presented as plaque-forming units per ml (pfu/ml). One-tailed Student's t test was used to calculate the p value, *$p < 0.05$, **$p < 0.005$. Error bars indicate ± SEM. LOD = limit of detection. See also Figure S2 and Table S1.

predicted (Figure S3). This viral population was subsequently administered into mice via footpad injection, and virus was isolated from total spleen 48 hr postinfection. Composition of amiRNAs present in viral populations was monitored through deep sequencing and revealed a clear enrichment of certain hairpins by the third mouse passage (Figure 3A). To determine if this enrichment was the direct result of the hairpin or a consequence of unrelated mutations elsewhere in the viral genome, we employed a genetic reset between passages three and four. The reset was accomplished by recloning the hairpins from passage three into the original viral genome, thereby ensuring no other

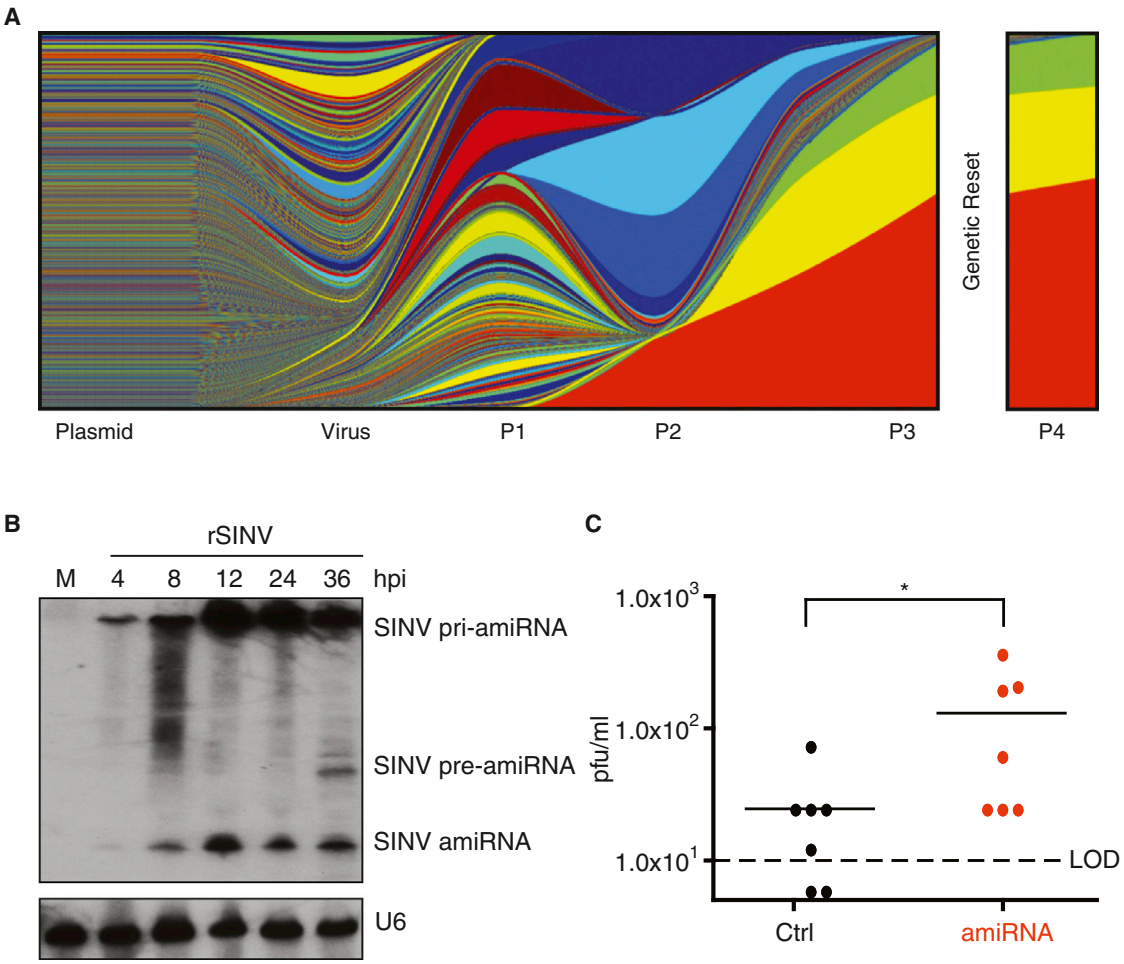

Figure 3. Monitored Enrichment of amiRNA during In Vivo Passages

(A) Matlab plot representing amiRNA viral hairpins present in the overall viral or plasmid populations. Each color depicts a unique amiRNA whose relative proportion corresponds to its abundance in the virus population at indicated passages (P). "Plasmid" depicts the hairpin diversity present in the SINV cDNA clones; "Virus" depicts hairpins present in the SINV amiRNA library, and "P1-P4" depicts hairpins identified in the spleen following each in vivo passage. Mice were infected with 5×10^6 plaque forming units (pfu) via footpad injection.

(B) Small RNA northern blot derived from cells infected with a recombinant Sindbis virus (rSINV) (moi = 1.0) encoding the most enriched amiRNA from (A). Blot analyzed for amiRNA and U6 expression.

(C) Virus titers derived from the spleens of mice infected via footpad injection with 5×10^5 pfu of either SINV-Ctrl or SINV-amiRNA and collected 48 hr post-infection. One-tailed Mann-Whitney U-test was used to calculate p value, n = 7, *$p < 0.05$. LOD = limit of detection. See also Figure S3.

mutations were present for the final passage. Upon readministering these three stains to naive mice, we found they maintained the same population dynamic, suggesting fitness enhancement correlated with amiRNA expression rather than unrelated genetic mutations (Figure 3A). Additionally, we determined optimal selection with three passages, as clear enrichment trends could be observed at this point. To further corroborate this idea, we again performed a genetic reset and generated a recombinant SINV expressing the most enriched amiRNA identified in this small screen (predicted to target USP32, a known ISG). Northern blot of cells infected with the recombinant virus demonstrated accurate processing and robust expression of this small RNA (Figure 3B). Furthermore, we compared virus growth of this amiRNA-containing-virus to a SINV encoding a nonspecific amiRNA (Figure 3C). As expected, incorporation of the amiRNA resulted in titers that were approximately one log higher than the control virus at 48 hr after in vivo infection (Figures 3C).

Large-Scale Genome Screening In Vivo to Identify Host/Virus Interactions

In an effort to conduct a more comprehensive, unbiased in vivo screen, we expanded the amiRNA virus library to approximately 10,000 unique hairpins and generated a second library of random barcodes that would not exert a selective advantage (Figures 4A and 4B). Using these two distinct libraries, we performed individual quadruplicate in vivo passaging sets and monitored the resulting eight populations by deep sequencing. Data were collected using four mice per passage per library, across three 48 hr infections. Barcoded or hairpin reads were consolidated and those viruses that represented at least 2% of

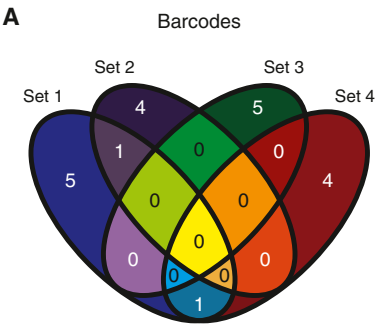

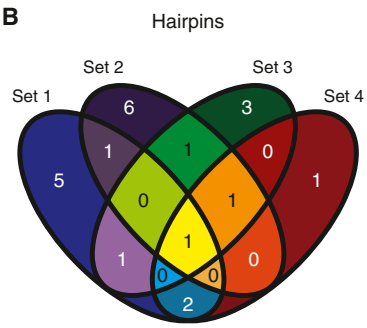

C

Barcodes

	4 Sets	3 Sets	2 Sets	1 Set
Total	0	0	2	20
Prop.	.00	.00	.005	.05

D

Hairpins

	4 Sets	3 Sets	2 Sets	1 Set
Total	1	2	8	22
Prop.	.01	.02	.08	.22

Figure 4. amiRNAs Confer a Reproducible Selection Advantage

(A and B) Venn diagrams depicting overlap of either barcoded (A) or amiRNA-expressing (B) viruses from four parallel in vivo screens. Shown are the number of viruses that make up more than 2% of the final viral population in each screen as determined by deep sequencing.

(C) Table of the number of clones found in at least 1, 2, 3, or 4 of the sets described in (A) as well as the proportion of each clone with respect to the total number of viruses present in the final passage.

(D) Same as (C) with respect to sets described in (B). See also Figure S4 and Table S2.

the total population were plotted (Figures 4A and 4B). These data demonstrated that only 0.5% of barcoded viruses could be identified as present in two sets with no barcoded strains being isolated in three or more (Figure 4C). In contrast, amiRNA-containing viruses showed a 16-fold enrichment for strains being found in two or more sets (Figure 4D and Table S2). Additionally, we could identify strains that were present in three or more independent sets. Not surprisingly, large cohorts of enriched amiRNAs targeted known ISGs and were annotated as virus response genes (Figure 5A). The only other two major categories of functionally grouped genes that demonstrated greater than 5-fold enrichment by passage three silenced factors involved in cellular homeostatis and general transcription (Figure 5A and Table S3).

Enriched amiRNAs Demonstrate Targeting and Alter Host Capacity to Limit Virus Replication

To independently corroborate the results of this in vivo screen, we determined the silencing potential of candidate amiRNAs that were identified in at least two independent sets. For each amiRNA, small RNA processing and expression by northern blot could be verified from both plasmid (Figure S4A) and SINV infection (Figures S4B and S4C). Furthermore, these same amiRNAs could be validated for silencing potential, and all but one resulted in a significant increase in virus titer when silenced with independently verified siRNAs (Figures S4D–S4J). To define the host factors that provided the most robust replicative advantage to the virus, we focused on the two hairpins that were enriched in three or more independent screens. Interestingly, both of these amiRNAs are predicted to target transcription factors implicated in self-renewal (Hu et al., 2009): Zinc finger protein X (amiRNA-Zfx) and the MAX gene-associated protein (amiRNA-Mga). Strikingly, Zfx and a factor sharing significant homology with Mga (Hurlin et al., 1999), Myc, have been demonstrated to share similar transcription factor occupancies involved in the regulation of genes related to cell cycle, cell death, and cancer (Chen et al., 2008; Hu et al., 2009). Notably, the subset of genes targeted by Zfx and Myc were found to include Stat1 (Chen et al., 2008; Hu et al., 2009), an essential transcription factor in the antiviral response (Levy and Darnell, 2002). Given the predominant selection for amiRNAs targeting genes involved in transcription (Figure 5A) and the apparent overlap between Zfx and Mga, we sought to further characterize how loss of either of these factors might impact the capacity for cells to limit virus replication.

Reduced Expression of Zfx and Mga Compromise the Cellular Host Antiviral Defense

To ensure that silencing of Mga could be directly implicated in conferring increased viral fitness, we independently targeted this host factor with an siRNA complementary to a unique region of the ORF (Figure S5A). Loss of Mga, independent of an amiRNA, produced a comparable phenotype, allowing SINV to replicate to one order of magnitude higher as compared to control siRNA (Figure S5B). In agreement with the depletion studies, we observed a corresponding decrease in viral replication following overexpression of Mga (Figure 5B). Moreover, loss of ISGs in the absence of Mga suggests that this transcription factor coordinates a critical role in the cellular response to virus infection (Figure 5C). This role for Mga was not restricted to SINV as we additionally observed comparable results upon infection with an attenuated influenza A virus, stimulation with double stranded RNA, or IFN-I treatment (Figure S5C). To corroborate Zfx's role in the antiviral response, we utilized primary fibroblasts from Zfx conditional knockout mice (Galan-Caridad et al., 2007). Comparable to the loss of Mga, genetic disruption of Zfx resulted in a 1.5 log increase in viral replication (Figure 5D). Additionally, loss of Zfx correlated with a dramatic reduction in ISGs, similar to the phenotype following Mga knockdown (Figure 5E). Taken together, these results suggest that Mga and Zfx are required to maintain a transcriptome capable of eliciting an effective response to virus replication.

In Vivo Screening Selects for Viruses Capable of Modulating Diverse Signaling Networks

To better understand why two relatively unknown factors were selected for their capacity to enhance replication, we investigated how each of the ORFs related to known antiviral pathways. To this end, we first investigated the transcriptional activity of the Ifnb gene in response to SINV following ctrl, Mga, or Zfx targeting (Figures S6A and S6B). These data revealed that loss of either Mga or Zfx resulted in a significant

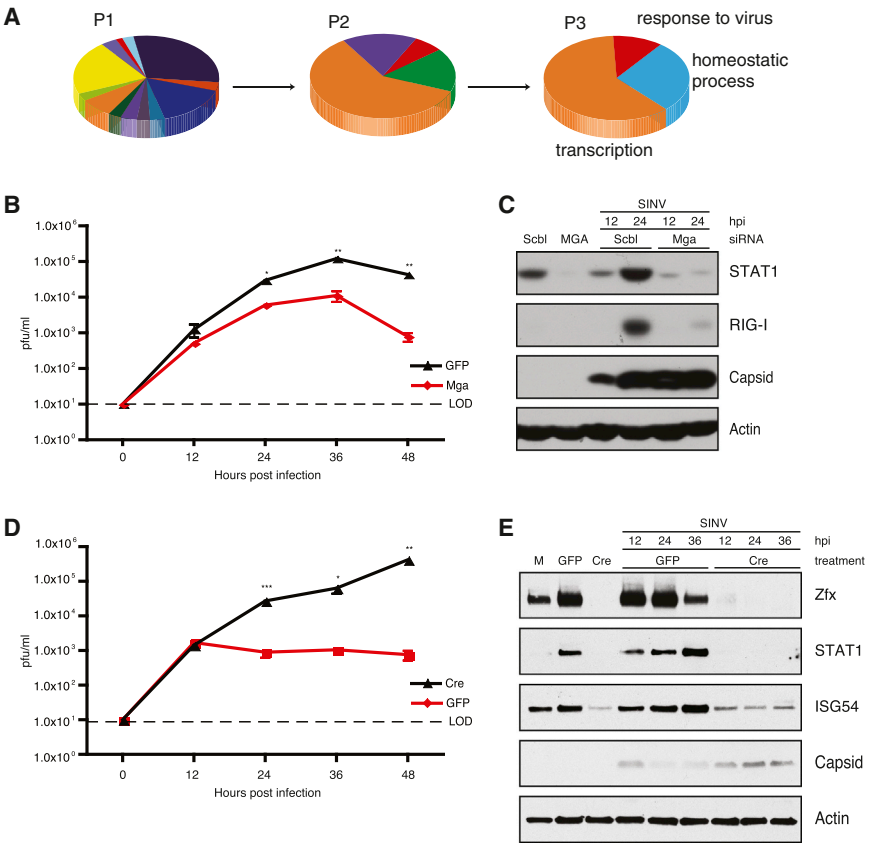

Figure 5. Mga and Zfx Aid in Coordinating the Antiviral Response

(A) Pie charts depicting gene function categories of predicted targets for every virus present at 0.01% or greater of the total populations in P1, P2, and P3.

(B) Multicycle growth curve of SINV performed in murine Hepa1.6 cells (moi = 0.01) and transfected with GFP or Mga expression plasmids.

(C) Western blot analysis of whole-cell extract derived from human lung bronchial epithelial cells (A549) treated with scrambled (ScbI) or Mga-targeting siRNAs and infected (48 hr post-transfection) with SINV (moi 0.1) and harvested. Blots depict RIG-I, STAT1, SINV capsid, and actin at the indicated time points.

(D) Multicycle growth curve of SINV-infected (moi 0.1) primary fibroblasts (*Zfx fl/fl*) treated with adeno-GFP or adeno-GFP/Cre and harvested at indicated time points.

(E) Western blot analysis of whole-cell extract derived from primary fibroblasts from (D). Blots depict Zfx, STAT1, SINV capsid, and actin. One-tailed Student's t test was used to calculate the p value and error bars denote ± SEM, $^{*}p < 0.05$, $^{**}p < 0.005$, and $^{***}p < 0.0005$. See also Figure S5 and Table S3.

reduction of IFNβ (Figure 6A). This phenotype is supported by loss of STAT1 at both the protein and RNA level (Figures 5C, 5E, and 6B). To further elucidate the molecular mechanism responsible for loss of IFNβ, we determined whether the IFN-I-dependent transcriptional induction of Stat1 was impacted by the loss of Mga and/or Zfx (Figure 6C). These data found that while the consequence of gene disruption resulted in comparable viral phenotypes and loss of IFN-I, the interruption of antiviral signaling was occurring at different stages in the signaling pathway. IFN-I-mediated upregulation of Stat1 was compromised only following knockdown of Mga (Figure 6C). These data implicate Mga in maintaining the capacity to respond to IFN-I. To determine the mechanism by which virus-induced *Ifnb* and *Stat1* is lost following Zfx knockdown, we analyzed NF-κB activity following TNF-α treatment (Figure 6D). These data implicated Zfx, but not Mga, in this cellular pathway. To better define the impact from loss of Mga and Zfx on the cellular transcriptome, we performed mRNA-Seq (Figures 6E and 6F and S6C and S6D). In agreement with the observed phenotype, these data demonstrated a dramatic decrease of the host machinery required for IFN-I and virus-induced signaling, suggesting this to be the cause for subsequent loss of IFN-I and ISG production (Table S4). Interestingly, loss of Zfx resulted in a dramatic loss of IKKβ (Ikbkb), the same virus-activated gene selected for in our in vitro studies (Figure S2A). Furthermore, siRNA treatment of Mga resulted in diminished levels of *Irf9*, *Stat2*, *Ifnar1*, *Ifnar2*, and perhaps most importantly, *Irf7*. It is also noteworthy that loss of Zfx and Mga both resulted in a significant reduction in RIG-I, also in agreement with our in vitro screens. Taken together, these data suggest that virus fitness may be defined by the ability of the pathogen to antagonize broad cellular responses rather than specific antiviral factors.

DISCUSSION

Here we describe a means by which to identify host factors required to maintain low levels of virus infection in the context of an in vivo model. Following the discovery that RNA viruses could be engineered to express miRNAs (Langlois et al., 2012; Rouha et al., 2010; Shapiro et al., 2010, 2012; Varble et al., 2010), we decided to exploit this activity and use it to perform siRNA screening in the hopes that it would aid in identifying aspects that control in vivo virus replication. This approach is unique compared to present strategies aimed at identifying similar interactions between host and pathogen in that standard siRNA screens demand nonphysiological infection models as they rely on cell culture. By enabling siRNA delivery through replication-competent RNA viruses, we can harness natural selection through siRNA production, allowing evolution to parse out those factors that are important in restricting natural infection regardless of cell type. Here we describe three such screens. First, we performed an in vitro screen to ascertain whether targeting virus-activated genes can enhance virus replication. This work identified RIG-I and IKKβ as important modulators of virus replication in cell culture. Following this proof-of-principle study, we investigated whether we could observe selection and enhanced replication in vivo using a significantly larger amiRNA library. Monitoring virus populations from this study revealed that

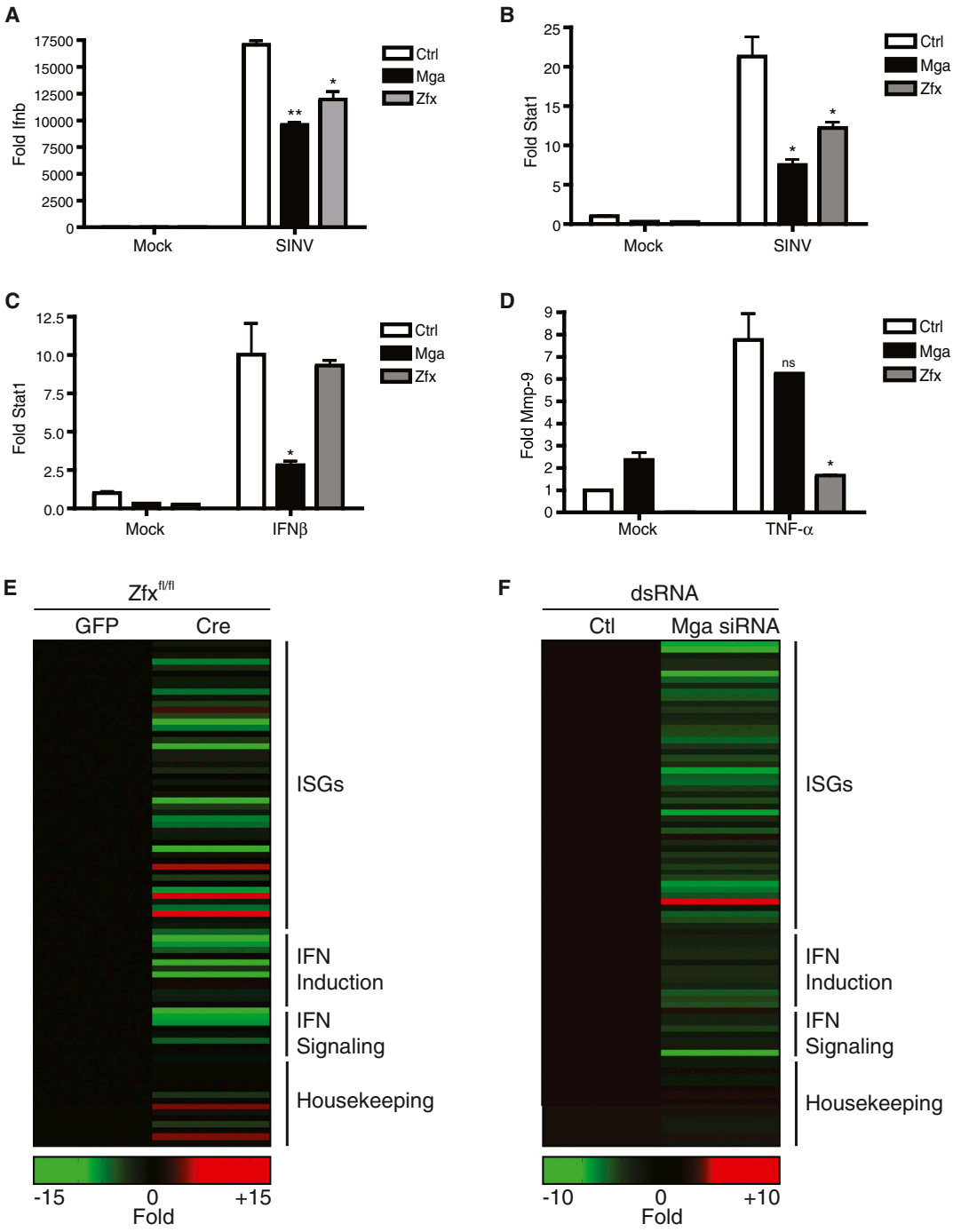

Figure 6. Zfx and Mga Perform Distinct Roles in Antiviral Signaling

(A) Quantitative real-time PCR (qPCR) analyses of RNA derived from A549 cells treated with scrambled (Scbl), Zfx, or Mga-targeting siRNAs and infected with SINV (moi = 2.0) and analyzed for Ifnb transcription.

(B) Same as (A) for Stat1.

(C) qPCR analysis of IFNβ-treated uninfected cells described in (A) and analyzed for Stat1.

(D) qPCR analysis of TNF-α-treated uninfected cells described in (A) and analyzed for Mmp-9. For all qPCR, Student's t test was used to calculate the p value and error bars denote ± SEM, *$p < 0.05$ and **$p < 0.005$.

(E) RNA-seq analysis on RNA extracted from primary fibroblasts (*Zfx fl/fl*) treated with adeno-GFP or adeno-GFP/Cre. Heatmap depicts fold change of genes as compared to adeno-GFP treatment. Genes were clustered into groups of IFN-stimulated genes (ISGs), genes responsible for IFN induction, IFN signaling, and housekeeping genes.

(F) RNA extracted from primary fibroblasts (E) treated with adeno-GFP, dsRNA, and Mga siRNA. Standard RNA-seq analysis was performed and analyzed as in (E). See also Figure S6 and Table S4.

selection could be observed and, similar to the in vitro screen, also identified genes previously implicated in the cellular response to virus infection. Last, we performed a large-scale screen to investigate selection in an unbiased manner. This work identified a combination of ISGs as well as factors involved in host transcription, including Zfx and Mga. Interestingly, loss of these factors resulted in a dramatic remodeling of the transcriptome and a loss of many antiviral genes including RIG-I and IKKβ.

It is noteworthy that this screen has a number of parameters that must be considered when evaluating the data. First, as the output of this screen is based on the emergence of dominant strains, it is biased toward the identification of siRNAs that provide an advantage following silencing only within an infected cell. Furthermore, these dynamics change with time, for example, if the IFN response has been induced, there is little advantage to silence PRRs. Moreover, as the characteristics of the hairpin population change over time, the relative fitness conferred by a hairpin may also fluctuate. In contrast, neutral hairpins, or those that cease to provide a benefit, should undergo counter selection. As SINV-mediated amiRNA production results in a low level of self-targeting (Shapiro et al., 2010), only those providing a net positive effect on viral fitness will be maintained throughout subsequent passages. In addition to the bias for viral effectors, current gaps in knowledge of siRNA silencing, coupled with the acute time frame of the viral infection, also impose some inherent constraints on this technological platform. For example, successful generation of an amiRNA does not always equate to significant knockdown of the target protein (Figure S1C). Conversely, off-target effects can complicate the function of a selected amiRNA, although this activity was not overtly apparent given our capacity to validate our top hits with knockout cells and independent siRNA experiments. In addition to siRNA dynamics, should protein half-life significantly exceed the viral life cycle, no advantage would be gained from cognate mRNA silencing. Factors such as these prevent absolute targeting of the transcriptome. Furthermore, it should be noted that the host factors identified by such a selection process would be influenced by the type of screen performed. For example, our proof-of-concept study here focused on increased virus titers from cell culture and splenic samples. However, as alphaviruses are neurotropic and elicit a unique immune response in the CNS (Griffin, 2003), intranasal inoculation followed by virus isolation in the brain may enrich for factors associated with crossing the blood-brain barrier in addition to a unique subset of host factors that enhance general replication. The capacity to perform such a screen with the same amiRNA library used in this study also illustrates the flexible nature of this technology to parse out an expansive list of virus/host interactions that are specific to a particular variable and/or pathogen.

Implicating host factors that contribute to the severity of a virus disease is essential in this new era of personal genomics (Everitt et al., 2012). In the context of an in vivo virus infection, our RNAi screen revealed two transcription factors as being important regulators of the host response to infection. Interestingly, mRNA-seq analyses of these two factors suggest that they may indirectly impact the overall cellular response to virus infection. However, it remains somewhat unclear how virus silencing of these two factors provides the time necessary to influence the host transcriptome in the context of a single round of infection. We speculate that loss of Mga or Zfx must rapidly diminish at least one critical factor in the first 6–8 hr of infection that results in the overall increase in virus titer. Such candidates include any component of the IFN-I signaling cascade that would prevent establishment of the antiviral state late in infection but could also include a potent ISG.

Another interesting observation that derives from this in vivo screen is the overall lack of ISGs identified. This may be due to the inherent ability of the virus to already antagonize these factors through Nsp2 function, thereby biasing the results to non-ISGs (Frolova et al., 2002). However, given that loss of specific ISGs could confer a growth advantage in our in vitro screen, this data may perhaps resonate the importance of some of the more universal host genes in controlling virus levels. In this regard, it would seem a successful strategy to enhance virus replication demands inducing a state of global cell deregulation. This concept is in fact the basis of how oncolytic viruses are thought to mediate replication specificity as transformation, by definition, demands compromising the signaling networks of a primary cell (Russell et al., 2012).

Despite the inherent limitations to this screen, the capacity to identify host factors in the context of the actual infection is invaluable. This screen permits bona fide virus replication as the output, as opposed to surface staining or a reporter assay, providing a more relevant and durable platform for identifying host factors. In all, this screening strategy takes advantage of multiple fundamental biological principles (RNAi, natural selection, and viral pathogenesis) to create a unique example of an in vivo RNAi screen to identify virus/host interactions. It should be noted that the knowledge obtained from this platform could in no way be used to enhance the pathogenesis of a virus found in nature. This is a result of the inherent attenuation that encoding a hairpin incurs (Shapiro et al., 2010) and is presumably the reason why RNA viruses do not naturally employ this strategy (Cullen, 2011). However, generating a library of equally attenuated viruses allows for selection of increased fitness only as it relates to that population. Applying this technology to future screens will undoubtedly identify factors responsible for virus replication, tropism, transmission, or persistence and result in a greater understanding of the interactions between virus and host.

EXPERIMENTAL PROCEDURES

Virus Design and Rescue

The SINV clones described were created by grafting hairpins, as described in Supplemental Experimental Procedures, into the TE12Q clone, a genetically modified strain containing a duplicate subgenomic mRNA promoter downstream of the structural genes (Cheng et al., 1996). MluI and NotI restriction sites were added to a preexisting BstEII site, and In-Fusion PCR cloning (Clontech Laboratories) was used to insert specified hairpins into SINV. The SINV miR-30 library, which is described elsewhere (Silva et al., 2005), was cloned into MluI and NotI via Infusion (Clontech) as per the manufacturer's instructions. Plasmid DNA encoding the SINV miR-30 library was subsequently transcribed using the mMessage mMachine SP6 Kit (Ambion), and 6 μg of RNA was transfected into 6×10^6 BHK-21 cells using the Nucleofector II machine (Lonza) and the Amaxa cell line Nucleofector Kit T reagent (Lonza). Rescued virus was harvested 48 hr posttransfection and titered for future use. Barcoded viruses were constructed by inserting 22 unique nucleotide barcodes into the BstEII site in the subgenomic region of SINV. The barcoded library was rescued and sequenced as described for the hairpin library. For in vitro

knockdown experiments, we utilized a mutant SINV encoding a proline-to-serine substitution at position 726 of nsP2 to enhance IFN production (Frolova et al., 2002). Rescue of these viruses were performed as described above. Control viruses (SINV ctrl) were comprised of either a nonfunctional amiRNA or miR-124, neither of which provides any growth advantage.

Cell Culture and Noninfectious Treatments

A549, Vero, BHK-21, Hepa 1.6, and murine embryonic fibroblast (MEF) cells were cultured in DMEM media supplemented with 10% FBS and 1% penicillin/streptomycin. RNA interference was performed using pools of oligonucleotides designed to target nothing (scbl), Zfx, or Mga (Santa Cruz Biotechnologies, sc-37007 and sc-89945, respectively). Life Technologies' silencer select siRNAs targeting Polr1A-s223665, MUC5AC-s9074, EPRS- s4767, RIG-I-s223614, and negative control #2-4390846 were used for SINV growth advantage experiments. A total of 50 pmols of RNA oligonucleotide pools were transfected into A549 and Hepa1.6 cells with Lipofectamine RNAiMAX (Invitrogen). Conditional Dicer1 MEFs (*Dcr1 fl/fl*) (Harfe et al., 2005) or Zfx fibroblasts (*Zfx fl/fl*) (Galan-Caridad et al., 2007) were infected with adenovirus expressing GFP or GFP-Cre (Vector Biolabs #1060 and #1700, respectively) at a multiplicity of infection (moi) of 125 and treated 4 days postinfection as described. IFN treatment was performed with recombinant universal IFNβ (R&D Systems) at a concentration of 100 units/ml. Transfection of the dsRNA mimetic (polyI:C, Sigma) was performed using 5 μg of polyI:C with Lipofectamine 2000 (Invitrogen) on 10E6 cells. TNF-α (GIBCO) was used at a concentration of 30 ng/ml. IFN and dsRNA treatments were performed at 10 hr and TNF-α at 24 hr. Plasmid transfections were performed using 4 μg of plasmid DNA with Lipofectamine 2000 (Invitrogen) on 10E6 cells and harvested 36–72 hr posttransfection. Plasmids expressing amiRNAs, GFP, or Mga are described elsewhere (Makeyev et al., 2007; Hurlin et al., 1999).

ISG Library

ISGs were selected based on previously published results (Schoggins et al., 2011; tenOever et al., 2007). The NCBI sequence of each gene was entered into http://biodev.extra.cea.fr/DSIR to generate 21 nt long siRNAs. The siRNAs were then ranked selected based on previously published guidelines for amiRNA design (Fellmann et al., 2011). The selected siRNA sequences were inserted into the mmu-miR-124-2 backbone, and SINVs were individually rescued and titered. Viruses were combined at equal titers to construct the library. A miR-124-expressing virus was included as a negative control.

Virus Infections

Viral infections were performed at the moi specified in the text. IAV infections were performed using the delta NS1 mutant previously described (García-Sastre et al., 1998). Virus was inoculated into indicated cell lines containing serum-free DMEM for 1 hr for SINV or PBS supplemented with 0.3% BSA (MP Biomedicals) and penicillin/streptomycin for IAV and collected at the indicated times. Multicycle growth curves were performed with SINV recombinants at indicated moi. A total of 0.1 ml of supernatant was removed at the indicated times. Supernatant was plaqued in Vero cells in serial dilutions in 2% methylcellulose. Plaques were counted 3 days postinfection.

Animal Infections

C57BL/6 4-week-old female mice were purchased from Taconic. Mice were anesthetized with 1:1:4.6 ketamine, xylazine, H_2O mixture then infected via footpad injection with 5×10^6 pfu, unless otherwise indicated. Spleens were harvested 48 hr postinfection and homogenized with 500 μl of PBS for either direct titering or propagation on BHK-21 cells and reinjection into mice for passaging experiments. All experiments involving animals were performed in accordance with Mount Sinai School of Medicine Institution of Animal Care and Use Committee.

Deep Sequencing and Data analysis of Virus Libraries

For deep sequencing analysis of small RNAs derived from the SINV library, samples were generated as previously described (Pfeffer et al., 2005). To monitor viral populations, Superscript II (Invitrogen) was used with random hexamers to generate cDNA, and then specific primers with barcoded Illumina linkers were used to amplify the amiRNA hairpin region. Deep sequencing samples were analyzed on the Illumina HiSeq 2000 sequencing platform. Using various shell scripts, the amiRNA backbone was stripped and distinct sequences were identified. Alignments were used to group sequences into "families" to control for sequencing error. These assigned IDs were kept constant throughout samples. Custom scripts in both shell and Perl were used to manage and analyze the data. A MySQL database was used to store and process the raw data. Selection experiments were visualized using Matlab. ISGs were defined as transcripts that increased by >2-fold according to GEO: GSE6837. Characterized targets were identified by determining the highest mean free energy (Mfe) targets to the predicted amiRNA, while excluding bulges and G:U base pairing in the seed region. Remaining targets were characterized en masse using highest Mfes as defined by RNAhybrid. Virus populations within each passage were annotated using DAVID Bioinformatics Resources as described (Huang da et al., 2009a, 2009b). Genes enriched by 5-fold or greater, for which GO annotations existed, are listed on Table S3.

mRNA-Seq Analysis

For mRNA-seq, mRNA was isolated from 1 μg of RNA using sera oligo-dT beads. Isolated RNA was used for cDNA synthesis with SuperScript II reverse transcriptase (Life Technologies). Samples then underwent second strand synthesis, end-repair, A-tailing, ligation, and PCR using the Illumina Truseq kit (Illumina, Cat. No1502062). Quality of amplified cDNA library was then tested using the Bioanalyzer DNA 1000 Assay. mRNA-seq libraries were clustered with cBOT (Illumina) and then run on HiSeq (Illumina) for 100 base single read sequencing. Reads were analyzed using a pipeline based on Bowtie and Samtools and aligned to the murine open reading frame database available from Ensembl Biomart (http://www.ensembl.org/). Individual genes were normalized as a percentage of total sample reads mapping to the reference genome.

Small RNA Northern Blot Analysis

Small RNA northern blots and probe labeling were performed as previously described (Pall and Hamilton, 2008). Probes used include: anti-miR-124, 5′-TGGCATTCACCGCGTGCCTTAA-3′; GFP-480, 5′-CGGCATCAAGGTGAACTTCAA-3′; GFP-440, 5′-ACAGCCACAACGTCTATATCA-3′; GFP-417, 5′-GCACAAGCTGGAGTACAACTA-3′; GFP-274, 5′-GGCTACGTCCAGGAGCGCACC-3′; GFP-122, 5′-TGCAAGCTGACCCTGAAGTTCA-3′; RIG-I, 5′-CTCCCGGACTTCGAACACGTTA-3′; amiRNA-USP32, 5′-TGGTGACAACAGTGGAAAGAAT-3′; amiRNA-Zfx, 5′-AGCCCACCTGGAGAGCCACAAA-3′; amiRNA-Mga, 5′-AGCCATATCTCTGCAGATGAAA-3′; amiRNA-ACAT1, 5′-CCCACTTTGAATGAAGTGGTTA-3′; amiRNA-MORC4, 5′-AGCAAAGGCTGCTGAGAAGAAA-3′; amiRNA-Pncr2, 5′-AGCTAATTATTTCATTGGCAAA-3′; and anti-U6, 5′-GCCATGCTAATCTTCTCTGTATC-3′.

Western Blot Analysis

Western blots were generated from total protein separated on a 7.5%–10% SDS-PAGE gel. Resolved protein was transferred to nitrocellulose (Bio-Rad), blocked for 1 hr with 5% skim milk at 25°C, and then incubated with the indicated antibody overnight at 4°C. Actin (Thermoscientific), Mga (Abcam), SINV Capsid (a kind gift from Dr. D. Griffin, Johns Hopkins), STAT1-C111 (Santa Cruz), RIG-I (a kind gift from Dr. A. Garcia-Sastre, MSSM), Zfx polyclonal (a kind gift from Dr. Boris Reizis), and the PR8 polyclonal antibody (a kind gift from Dr. P. Palese, MSSM) antibodies were all used at a concentration of 1 μg/ml in 5% skim milk. Secondary mouse and rabbit antibodies (GE Healthcare) were used at a 1:5,000 dilution for 1 hr at 25°C. Immobilon Western Chemiluminescent HRP Substrate (Millipore) was used as directed.

Statistical Analysis

All plaque assays and growth curves were determined in three biological replicates and plaqued in two technical replicates unless otherwise indicated. One-tailed Student's t tests were performed on biological replicates to determine significance unless otherwise indicated. Luciferase assays were performed in three biological replicates. One-tailed Student's t tests were performed on biological replicates to determine significance. qPCR analysis was performed in two biological replicates and analyzed in two technical replicates unless otherwise indicated. One-tailed Student's t tests were performed on biological replicates to determine significance.

qPCR Analysis

Conventional qPCR was performed on indicated cDNA samples using KAPA SYBR FAST qPCR Master Mix (KAPA biosystems). Delta delta cycle thresholds were calculated using tubulin as the endogenous housekeeping gene and mock treated cells as the calibrator in respective experiments. Primers used include: mRIG-I, 5′- AAGAGCCAGAGTGTCAGAATCT-3′ and 5′-AGCTCCAGTTGGTAATTTCTTGG-3′; hStat1, 5′-CTTCTCTGGCGACAGTTTTC-3′ and 5′-CCTTTCAATTTTACCTTCAG-3′; hactin, 5′-ACTGGAACGGTGAAGGTGAC-3′ and 5′-GTGGACTTGGGAGAGGACTG-3′; ma-tubulin, 5′-TGCCTTTGTGCACTGGTATG-3′ and 5′-CTGGAGCAGTTTGACGACAC-3′; hMmp-9, 5′-CTTTGAGTCCGGTGGACGAT-3′ and 5′-TCGCCAGTACTTCCCATCCT-3′; hZfx, 5′-TTGCTGAAATCGCTGACGAAG-3′ and 5′-GCAATCGGCATGAAGGTTTTGAT-3′; mZfx, 5′- GCAGTGCATGAACAGCAAGT-3′ and 5′-GCAAGGTGTTCAGGATGGTT-3′; hMga, 5′- AGGAGCACGTGGACATTGAG-3′ and 5′-TTGGTGGAGCCTTTCGACTC-3′; mMga, 5′- GGCCAATTGAAAATGCCCCT-3′ and 5′-GTAGGAGAACCCTGCTGCAC-3′; hIFNb, 5′-GTCAGAGTGGAAATCCTAAG-3′ and 5′-ACAGCATCTGCTGGTTGAAG-3′.

Luciferase Assay

BHKs were transfected with Gaussian luciferase constructs containing the indicated target sites, untargeted firefly luciferase, and a plasmid expressing the indicated hairpin. Where applicable, BHKs were infected 2 hr posttransfection at an moi of three. Twelve hours posttransfection or 18 hr postinfection, medium was replaced with serum-free DMEM. Four hours after media change, luciferase expression was determined as per the manufacturer's instructions (Promega), with levels normalized to firefly luciferase and the untargeted control.

SUPPLEMENTAL INFORMATION

Supplemental Information includes six figures, four tables, and Supplemental Experimental Procedures and can be found with this article online at http://dx.doi.org/10.1016/j.chom.2013.08.007.

ACKNOWLEDGMENTS

This material is based upon work supported in part by the US Army Research Laboratory and the US Army Research Office under grant numbers W911NF-12-R-0012 and W911NF-08-1-0413. BtO is supported in part by the Burroughs Wellcome Fund. We also wish to thank Drs. B. Reizis (Columbia), R. Eisenman (Fred Hutchinson Cancer Research Center), D. Griffin (Johns Hopkins), A. Garcia-Sastre (MSSM), and P. Palese (MSSM) for the Zfx knockout fibroblasts, cDNA expression vector for Mga, SINV Capsid antibody, RIG-I antibody and Ddx58 knockout fibroblasts, and IAV antibody, respectively. Next-generation sequencing was performed by the Genomics Core Facility, Icahn Institute for Genomics and Multiscale Biology at Mount Sinai.

Received: April 24, 2013
Revised: July 8, 2013
Accepted: August 15, 2013
Published: September 11, 2013

REFERENCES

Bartel, D.P. (2004). MicroRNAs: genomics, biogenesis, mechanism, and function. Cell *116*, 281–297.

Brass, A.L., Dykxhoorn, D.M., Benita, Y., Yan, N., Engelman, A., Xavier, R.J., Lieberman, J., and Elledge, S.J. (2008). Identification of host proteins required for HIV infection through a functional genomic screen. Science *319*, 921–926.

Chen, X., Xu, H., Yuan, P., Fang, F., Huss, M., Vega, V.B., Wong, E., Orlov, Y.L., Zhang, W., Jiang, J., et al. (2008). Integration of external signaling pathways with the core transcriptional network in embryonic stem cells. Cell *133*, 1106–1117.

Cheng, E.H., Levine, B., Boise, L.H., Thompson, C.B., and Hardwick, J.M. (1996). Bax-independent inhibition of apoptosis by Bcl-XL. Nature *379*, 554–556.

Cullen, B.R. (2011). Viruses and microRNAs: RISCy interactions with serious consequences. Genes Dev. *25*, 1881–1894.

Everitt, A.R., Clare, S., Pertel, T., John, S.P., Wash, R.S., Smith, S.E., Chin, C.R., Feeley, E.M., Sims, J.S., Adams, D.J., et al.; GenISIS Investigators; MOSAIC Investigators. (2012). IFITM3 restricts the morbidity and mortality associated with influenza. Nature *484*, 519–523.

Fellmann, C., Zuber, J., McJunkin, K., Chang, K., Malone, C.D., Dickins, R.A., Xu, Q., Hengartner, M.O., Elledge, S.J., Hannon, G.J., and Lowe, S.W. (2011). Functional identification of optimized RNAi triggers using a massively parallel sensor assay. Mol. Cell *41*, 733–746.

Ferris, M.T., Aylor, D.L., Bottomly, D., Whitmore, A.C., Aicher, L.D., Bell, T.A., Bradel-Tretheway, B., Bryan, J.T., Buus, R.J., Gralinski, L.E., et al. (2013). Modeling host genetic regulation of influenza pathogenesis in the collaborative cross. PLoS Pathog. *9*, e1003196.

Frolova, E.I., Fayzulin, R.Z., Cook, S.H., Griffin, D.E., Rice, C.M., and Frolov, I. (2002). Roles of nonstructural protein nsP2 and Alpha/Beta interferons in determining the outcome of Sindbis virus infection. J. Virol. *76*, 11254–11264.

Galan-Caridad, J.M., Harel, S., Arenzana, T.L., Hou, Z.E., Doetsch, F.K., Mirny, L.A., and Reizis, B. (2007). Zfx controls the self-renewal of embryonic and hematopoietic stem cells. Cell *129*, 345–357.

García-Sastre, A., Egorov, A., Matassov, D., Brandt, S., Levy, D.E., Durbin, J.E., Palese, P., and Muster, T. (1998). Influenza A virus lacking the NS1 gene replicates in interferon-deficient systems. Virology *252*, 324–330.

Griffin, D.E. (2003). Immune responses to RNA-virus infections of the CNS. Nat. Rev. Immunol. *3*, 493–502.

Harfe, B.D., McManus, M.T., Mansfield, J.H., Hornstein, E., and Tabin, C.J. (2005). The RNaseIII enzyme Dicer is required for morphogenesis but not patterning of the vertebrate limb. Proc. Natl. Acad. Sci. USA *102*, 10898–10903.

Hu, G., Kim, J., Xu, Q., Leng, Y., Orkin, S.H., and Elledge, S.J. (2009). A genome-wide RNAi screen identifies a new transcriptional module required for self-renewal. Genes Dev. *23*, 837–848.

Huang da, W., Sherman, B.T., and Lempicki, R.A. (2009a). Bioinformatics enrichment tools: paths toward the comprehensive functional analysis of large gene lists. Nucleic Acids Res. *37*, 1–13.

Huang da, W., Sherman, B.T., and Lempicki, R.A. (2009b). Systematic and integrative analysis of large gene lists using DAVID bioinformatics resources. Nat. Protoc. *4*, 44–57.

Hurlin, P.J., Steingrìmsson, E., Copeland, N.G., Jenkins, N.A., and Eisenman, R.N. (1999). Mga, a dual-specificity transcription factor that interacts with Max and contains a T-domain DNA-binding motif. EMBO J. *18*, 7019–7028.

Kincaid, R.P., Burke, J.M., and Sullivan, C.S. (2012). RNA virus microRNA that mimics a B-cell oncomiR. Proc. Natl. Acad. Sci. USA *109*, 3077–3082.

Kolakofsky, D., Kowalinski, E., and Cusack, S. (2012). A structure-based model of RIG-I activation. RNA *18*, 2118–2127.

König, R., Zhou, Y., Elleder, D., Diamond, T.L., Bonamy, G.M., Irelan, J.T., Chiang, C.Y., Tu, B.P., De Jesus, P.D., Lilley, C.E., et al. (2008). Global analysis of host-pathogen interactions that regulate early-stage HIV-1 replication. Cell *135*, 49–60.

König, R., Stertz, S., Zhou, Y., Inoue, A., Hoffmann, H.H., Bhattacharyya, S., Alamares, J.G., Tscherne, D.M., Ortigoza, M.B., Liang, Y., et al. (2010). Human host factors required for influenza virus replication. Nature *463*, 813–817.

Krishnan, M.N., Ng, A., Sukumaran, B., Gilfoy, F.D., Uchil, P.D., Sultana, H., Brass, A.L., Adametz, R., Tsui, M., Qian, F., et al. (2008). RNA interference screen for human genes associated with West Nile virus infection. Nature *455*, 242–245.

Langlois, R.A., Shapiro, J.S., Pham, A.M., and tenOever, B.R. (2012). In vivo delivery of cytoplasmic RNA virus-derived miRNAs. Mol. Ther. *20*, 367–375.

Levy, D.E., and Darnell, J.E., Jr. (2002). Stats: transcriptional control and biological impact. Nat. Rev. Mol. Cell Biol. *3*, 651–662.

Li, Q., Brass, A.L., Ng, A., Hu, Z., Xavier, R.J., Liang, T.J., and Elledge, S.J. (2009). A genome-wide genetic screen for host factors required for hepatitis C virus propagation. Proc. Natl. Acad. Sci. USA *106*, 16410–16415.

Li, J., Ding, S.C., Cho, H., Chung, B.C., Gale, M., Jr., Chanda, S.K., and Diamond, M.S. (2013). A short hairpin RNA screen of interferon-stimulated genes identifies a novel negative regulator of the cellular antiviral response. MBio *4*, e00385–e13.

Loo, Y.M., and Gale, M., Jr. (2011). Immune signaling by RIG-I-like receptors. Immunity *34*, 680–692.

Makeyev, E.V., Zhang, J., Carrasco, M.A., and Maniatis, T. (2007). The MicroRNA miR-124 promotes neuronal differentiation by triggering brain-specific alternative pre-mRNA splicing. Mol. Cell *27*, 435–448.

McWhirter, S.M., Tenoever, B.R., and Maniatis, T. (2005). Connecting mitochondria and innate immunity. Cell *122*, 645–647.

Pall, G.S., and Hamilton, A.J. (2008). Improved northern blot method for enhanced detection of small RNA. Nat. Protoc. *3*, 1077–1084.

Parameswaran, P., Sklan, E., Wilkins, C., Burgon, T., Samuel, M.A., Lu, R., Ansel, K.M., Heissmeyer, V., Einav, S., Jackson, W., et al. (2010). Six RNA viruses and forty-one hosts: viral small RNAs and modulation of small RNA repertoires in vertebrate and invertebrate systems. PLoS Pathog. *6*, e1000764.

Perez, J.T., Pham, A.M., Lorini, M.H., Chua, M.A., Steel, J., and tenOever, B.R. (2009). MicroRNA-mediated species-specific attenuation of influenza A virus. Nat. Biotechnol. *27*, 572–576.

Pfeffer, S., Zavolan, M., Grässer, F.A., Chien, M., Russo, J.J., Ju, J., John, B., Enright, A.J., Marks, D., Sander, C., and Tuschl, T. (2004). Identification of virus-encoded microRNAs. Science *304*, 734–736.

Pfeffer, S., Sewer, A., Lagos-Quintana, M., Sheridan, R., Sander, C., Grässer, F.A., van Dyk, L.F., Ho, C.K., Shuman, S., Chien, M., et al. (2005). Identification of microRNAs of the herpesvirus family. Nat. Methods *2*, 269–276.

Rouha, H., Thurner, C., and Mandl, C.W. (2010). Functional microRNA generated from a cytoplasmic RNA virus. Nucleic Acids Res. *38*, 8328–8337.

Russell, S.J., Peng, K.W., and Bell, J.C. (2012). Oncolytic virotherapy. Nat. Biotechnol. *30*, 658–670.

Schilte, C., Couderc, T., Chretien, F., Sourisseau, M., Gangneux, N., Guivel-Benhassine, F., Kraxner, A., Tschopp, J., Higgs, S., Michault, A., et al. (2010). Type I IFN controls chikungunya virus via its action on nonhematopoietic cells. J. Exp. Med. *207*, 429–442.

Schoggins, J.W., Wilson, S.J., Panis, M., Murphy, M.Y., Jones, C.T., Bieniasz, P., and Rice, C.M. (2011). A diverse range of gene products are effectors of the type I interferon antiviral response. Nature *472*, 481–485.

Sessions, O.M., Barrows, N.J., Souza-Neto, J.A., Robinson, T.J., Hershey, C.L., Rodgers, M.A., Ramirez, J.L., Dimopoulos, G., Yang, P.L., Pearson, J.L., and Garcia-Blanco, M.A. (2009). Discovery of insect and human dengue virus host factors. Nature *458*, 1047–1050.

Shapiro, J.S., Varble, A., Pham, A.M., and tenOever, B.R. (2010). Noncanonical cytoplasmic processing of viral microRNAs. RNA *16*, 2068–2074.

Shapiro, J.S., Langlois, R.A., Pham, A.M., and tenOever, B.R. (2012). Evidence for a cytoplasmic microprocessor of pri-miRNAs. RNA *18*, 1338–1346.

Silva, J.M., Li, M.Z., Chang, K., Ge, W., Golding, M.C., Rickles, R.J., Siolas, D., Hu, G., Paddison, P.J., Schlabach, M.R., et al. (2005). Second-generation shRNA libraries covering the mouse and human genomes. Nat. Genet. *37*, 1281–1288.

Takeuchi, O., and Akira, S. (2008). MDA5/RIG-I and virus recognition. Curr. Opin. Immunol. *20*, 17–22.

tenOever, B.R. (2013). RNA viruses and the host microRNA machinery. Nat. Rev. Microbiol. *11*, 169–180.

tenOever, B.R., Ng, S.L., Chua, M.A., McWhirter, S.M., García-Sastre, A., and Maniatis, T. (2007). Multiple functions of the IKK-related kinase IKKepsilon in interferon-mediated antiviral immunity. Science *315*, 1274–1278.

Varble, A., Chua, M.A., Perez, J.T., Manicassamy, B., García-Sastre, A., and tenOever, B.R. (2010). Engineered RNA viral synthesis of microRNAs. Proc. Natl. Acad. Sci. USA *107*, 11519–11524.

Vignuzzi, M., Stone, J.K., Arnold, J.J., Cameron, C.E., and Andino, R. (2006). Quasispecies diversity determines pathogenesis through cooperative interactions in a viral population. Nature *439*, 344–348.

Zeng, Y., Wagner, E.J., and Cullen, B.R. (2002). Both natural and designed micro RNAs can inhibit the expression of cognate mRNAs when expressed in human cells. Mol. Cell *9*, 1327–1333.